Design of 3D-Printed Soft Pneunet Actuator for Robotic Fruit Harvesting

By
Lissette Wilhelm

A THESIS

submitted to

Oregon State University

Honors College

in partial fulfillment of
the requirements for the
degree of

Honors Baccalaureate of Science in Mechanical Engineering
(Honors Scholar)

Presented 9 March 2022
Commencement June 2022

AN ABSTRACT OF THE THESIS OF

Lissette Wilhelm for the degree of Honors Baccalaureate of Science in Mechanical Engineering presented on 9 March 2022. Title:
Design of 3D-Printed Soft Pneunet Actuator for Robotic Fruit Harvesting

Abstract approved:

____

Joe Davidson

This work details the development of 3D printed Thermoplastic Urethane (TPU) pneunet actuators for use in apple picking for agricultural soft robotics. These actuators increase the force capabilities of soft pneunets and simplify manufacturing. Grippers based on these actuators are ideal for apple picking because they are compliant, yet exert sufficient force to pull ripe apples from branches. The pneunets are printed in Cheetah TPU with an interior chamber size to wall thickness ratio of 2 mm to 1 mm, respectively. The actuators were optimized for a maximum pull force of 23 N which, when combined in a three-finger grip, can provide up to 69 N of pulling force. The block force test revealed a maximum force output of 22.77 N $\pm$ 1.41. The radius of curvature test revealed a minimum radius of curvature of 22.41 with the medium finger at a pressure of 30 psi which can grasp apples from 65.4 mm to 75.0 mm in diameter. The actuators can be combined into a gripper with a minimum of 3 actuators. This type of gripper could enable apple harvesting while maintaining compliance for protecting the fruit from bruising. Future work includes assembling the pneunets into a three-actuator gripper.

Key Words: Pneunet, TPU, Actuator, Soft Robotics, Three Dimensional (3D) Printing

Corresponding e-mail address: wilhelli@oregonstate.edu

Design of 3D-Printed Soft Pneunet Actuator for Robotic Fruit Harvesting

By
Lissette Wilhelm

A THESIS

submitted to

Oregon State University

Honors College

in partial fulfillment of
the requirements for the
degree of

Honors Baccalaureate of Science in Mechanical Engineering
(Honors Scholar)

Presented 9 March 2022
Commencement June 2022

Honors Baccalaureate of Science in Mechanical Engineering project of Lissette Wilhelm presented on 9 March 2022.

APPROVED:

Joe Davidson, Mentor, representing Mechanical, Industrial, and Manufacturing Engineering

Steph Walker, Committee Member, representing Mechanical, Industrial, and Manufacturing Engineering

Cindy Grimm, Committee Member, representing Mechanical, Industrial, and Manufacturing Engineering

Toni Doolen, Dean, Oregon State University Honors College

I understand that my project will become part of the permanent collection of Oregon State University Honors College. My signature below authorizes release of my project to any reader upon request.

Lissette Wilhelm, Author

Contents

List of Figures

Acronym Dictionary

3D Three Dimensional. 2

3D three dimensional. 1, 3, 4, 6, 10, 13

CAD Computer Aided Design. 6

FDM Fused Deposition Modeling. 3

TPU Thermoplastic Urethane. 1–3, 6, 7, 13, 14

1 Introduction

Fruit harvesting is a dull and dirty activity which makes it a reasonable job for robot fruit pickers. Robots can perform repetitive tasks without fatigue. Apple picking robots typically consist of a robotic arm with an end effector attached. The robotic arm will use vision processing to locate apples and sensors in the end effector to determine the success of the apple picking. Some apple grippers use hard robotic end effectors made of metal with a cutter to disconnect the stem from the branch [1]. Other apple grippers involve a gripper to gently grab the apple and pull it from the branch [2] [3]. A plum gripper uses grippers in different orientations to pick plums [4].

Soft robotics offers material compliance that hard robotics often lacks, which makes it desirable for fruit picking. Soft robotics typically uses soft elastomeric materials (or a blend of hard and soft materials) to perform tasks otherwise difficult to achieve in hard robotics. Soft actuators are often made to mimic structures like octopus arms, caterpillars, and elephant trunks [5]. These actuators can use air or water as a means of actuation. In this work, water is used to fill a structure called a pneunet to achieve bending [6]. The movement of this water causes the actuator itself to dynamically change the form, allowing the actuator to accomplish the bending in a predetermined direction. The compliance of materials used in soft robotics allows actuators like this to grip irregularly shaped objects [7]. These characteristics make pneunets a good solution for harvesting fruit or performing other nuanced repetitive motion tasks because they are modular and compliant [7].

This paper will discuss the manufacturing, testing, and performance of pneunet actuators for apple picking. Based on previous work by Jun Li [8], the combination of the actuators needs a maximum grasping force of 37.5 N so the actuators built as part of Jun Li's research were designed to withstand a minimum blocked force test of 12.5 N. The actuators for this paper were three dimensional (3D) printed with a compliant yet firm Thermoplastic Urethane (TPU) filament with a shore hardness of 85A. Three sizes of pneunet actuators were designed and created with varying chamber cross-sectional areas to determine the best size of actuator for a desired apple picking force of 30 N. Blocked force tests were performed on all three actuators at pressures from 15-40 psi to determine the force output at each actuation pressure. The radius of curvature tests was performed to determine the range of curvatures possible from 15-40 psi. Blocked force and curvature data are analyzed in the context of the quality of an apple picking grasp.

2 Prior Work

Pneunets were chosen due to their compliant finger-like structure for manipulation. Other gripping solutions for apple picking tasks could include wrap-around and granular jamming, however, pneunets are easily structured to replicate human hands [4] [9] [10]. There are smaller silicone grippers for smaller fruits like plums which can grab fruit in different orientations that apple grippers cannot because of the stem and force required to remove the fruit [4]. Another option for fruit picking is a pneumatic enveloping gripper with a tube-like structure, that engulfs and applies equal pressure to the fruit [9]. Unfortunately, this wrap-around structure solution is currently too small to house an apple and even if the gripper was big enough, the gripper would need to maintain constant pressure to correctly grasp the apple [9]. Another form of enveloping gripper is the origami magic ball [11] which is a similar soft gripper that uses suction to grasp objects. Particle jamming may be useful for apple picking, however current literature addressing jamming for the use of apple picking demonstrates that the forces may be too low to pull an apple from the stem [9]. For example, one particle jamming gripper could only reach a force of 8.4 N [10].

An apple-picking gripper needs to resist a pulling force of at least 30 N [12]. One investigating study [8] determined the maximum grasping force required to be 37.52 (three actuators total).

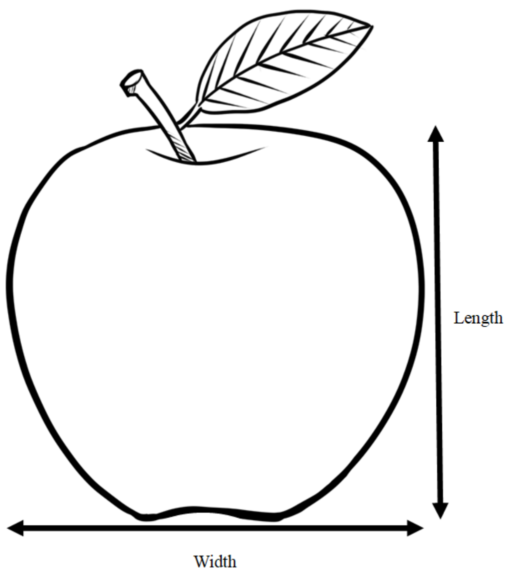

Figure 1: The length and width definitions are shown on an apple.

The wide variety of apple cultivars have different dimensions and additional complexity for an automated apple harvester. Apples have different sizes based on the apple variety. The length and width definitions are displayed in Figure 1. One research work [8] the Gala apple had the smallest length of all species tested, from stem to calyx (64.99 mm) and a Pink Lady apple had the longest length of 79.49 mm. Width also varies - Envy apples have the largest width of 80.0 mm and Jazz apples have the shortest width of 66.1 mm [12]. We used these apple lengths as reference values when designing the actuators[12].

Figure 2: The figure is an example of a silicone pneunet fully bent [13].

As seen in Figure 2, pneunets are a form of soft actuator with chambers connected by a tunnel that collectively determine the properties of the actuator [7] [14] [13]. When the pneunet is filled with fluid, it inflates like a balloon which causes the actuator to curl. Pneunet walls require a delicate balance between stiffness and impermeability [15]. If the walls are too thick, the actuator won't move due to the stiffness. If the walls are too thin, air can escape which renders the actuator useless. Equations can be used to estimate the force output of silicone pneunets, however, they require test data [13]. Some pneunets have a rougher base to generate more friction when gripping objects [16]. The compliance of the material used to make the actuator, when pressed into an apple, reduces the likelihood of bruised fruit. 3D printing offers a simple solution for manufacturing these actuators in one piece with customizable sizes.

Fused Deposition Modeling (FDM) is a form of 3D printing that extrudes melted thermoplastic material layers together using a heated nozzle and deposits the melted material layer by layer to form a 3D shape. The thermoplastic layers are fused together which allows the user to create a complete part with a model, including grippers such as pneunets [7] [14]. TPU filament is a softer material than traditional 3D printing thermoplastics (60-90 values of shore hardness [17]) and is useful for 3D printing compliant parts. TPU 3D printing requires a heated build chamber to maintain a constant temperature on all parts of the printed model; otherwise, holes and imperfections may develop. This is especially important for pneunets, where escaping air means failure of the actuator [7]. Cheetah filament, a TPU material by NinjaTek with a shore hardness of 85A, was used for all actuator prints.

3 Materials and Methods

3.1 Pneunet Actuator Design

Pneunets can be designed in multiple configurations [15]. The pneunets used in this paper are rectangular in shape, which was found to offer the best cross of strength and flexibility [15]. A rounded rectangular pneunet is another rectangular pneunet shape with a curved chamber top. It was considered for this work, however, it was non-ideal for the 3D printing process because the excess material made the actuator stiffer and less likely to flex around an object. The 3D printer also has to deposit more material for a rounded edge than a squared edge which restricts bending of the actuator. The non-rounded rectangular shape can be found in Figure 3a and the rounded rectangular shape can be found in Figure 3b.

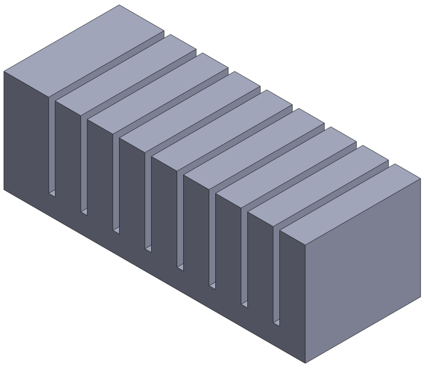

(a) The rectangular pneunet shape.

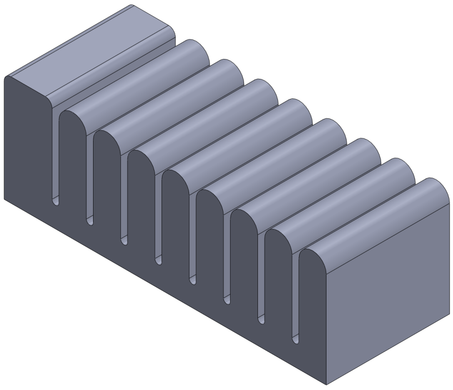

(b) The rounded rectangular pneunet shape.

Figure 3: The figure is a comparison between the rectangular pneunet and the rounded rectangular pneunet.

The measurements in Figure 4 are shown in Table 1. The length of the actuators is designed to wrap around an apple with a length of 72 mm and a width of 73 mm. Three pneunet actuator sizes was created each with a different chamber cross-sectional area. The length of all three actuators were the same since apples range in width from 80.0 mm to 66.1 mm [12]. An apple with a width of 70 mm and a height of 67 mm is included in Figure 5 for scale. The cross-sectional area of the small pneunet was chosen to emulate a human finger [15]. The small pneunet has a cross-sectional area of 18 mm by 16 mm. The medium pneunet has a cross-sectional area of 28 mm by 28 mm. The large pneunet has a cross-sectional area of 50 mm by 50 mm. The cross-sectional area of the chambers was incrementally increased to increase force output for the actuators. All three actuators are 116 mm long with 23 chambers. The interior of the chambers is 2 mm in length with 1 mm walls to contain the air. The space between each ridge is 1mm.

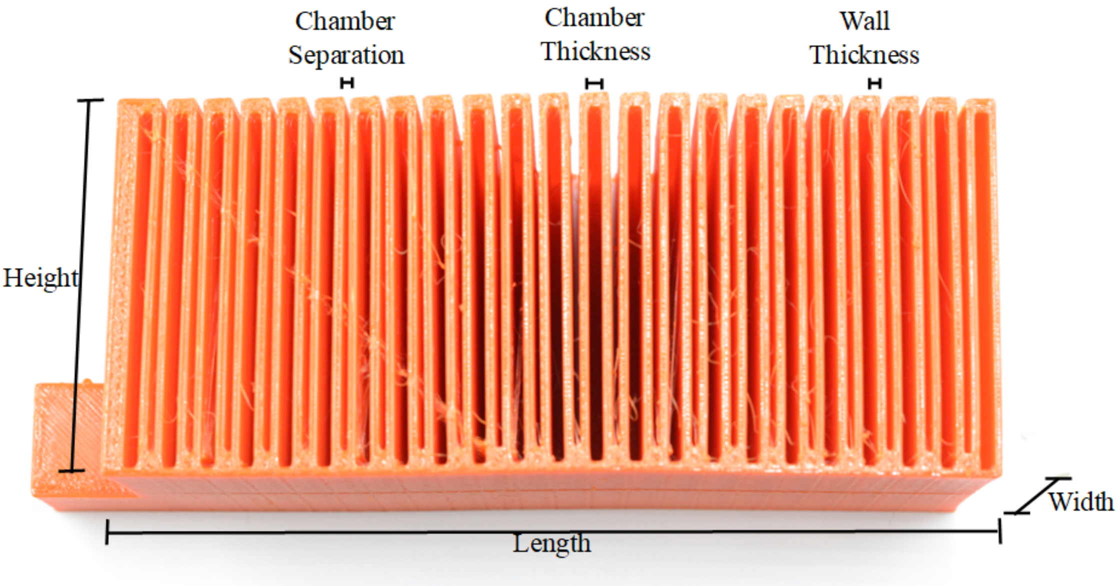

Figure 4: The dimensions of the pneunets depict the definitions discussed.

	Small	**Medium**	**Large**
Length	116	116	116
Width	18	28	50
Height	16	28	50
Wall Thickness	1	1	1
Chamber Thickness	2	2	2
Chamber Separation	1	1	1
Number of Chambers	23	23	23

Table 1: The dimensions of the three sizes of actuators in millimeters.

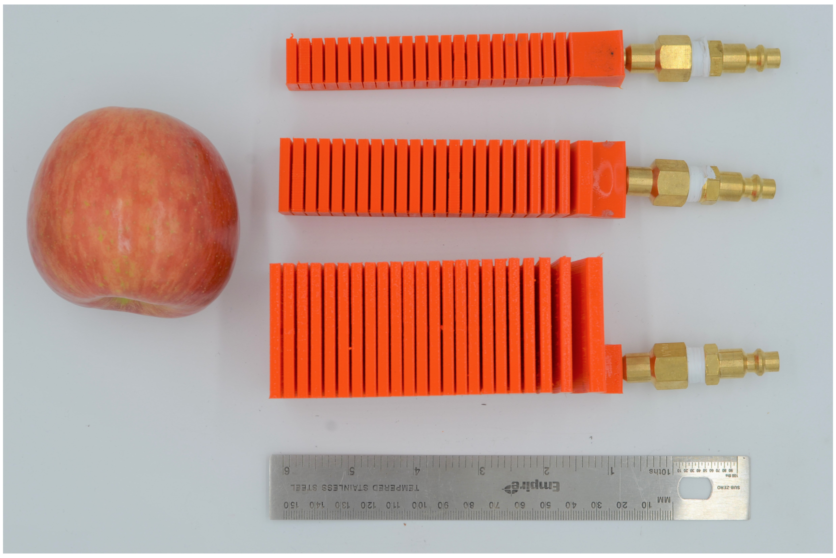

Figure 5: The three actuators are compared to the size of an apple.

3.2 3D Printing Process

3.2.1 TPU Printing Process

Cheetah TPU filament (Shore Hardness 85A. NinjaTek) was printed on a Prusa MK3S printer with an enclosure [18] [7]. Printing parameters were as follows: 0.3 mm layer height, 100% rectilinear infill, 240 °C nozzle temperature, and 50 °C bed temperature. Gianni Stano [15] advised printing pneunets with a line width above 0.2 mm which proved effective. The Computer Aided Design (CAD) models are printed at 100% rectilinear infill to ensure proper layer adhesion. The rectilinear pattern allows the extruder to continuously follow the rectangular shape of the actuators, which is critical for ensuring no air holes are formed. On the 3D printing extruder, the retractor knob needs to be loosened to its minimum holding force before printing; otherwise, the filament can stretch and cause the extruder to stop pulling the new filament, or the filament will be fed too aggressively into the hot-end of the printer causing the filament to jam.

Ensuring the nozzle remains in contact with the part at all times is critical to the print quality. Proper bonding of material in all areas prevents air holes from forming. Two different methods of heat treatment were tested to improve layer bonding after print completion. The first method, annealing, uses a heat gun to help the exterior of the print. The second method, ironing, uses the hot 3D printing nozzle to run along the top of the completed print to improve surface finish. Annealing the TPU increases its shore hardness and makes it less compliant [19]. Ironing the top layer of the prints with the nozzle was also attempted, it resulted in a weaker top layer with more holes. Extra materials gathered on the nozzle created holes where air could enter between the exterior walls of the chamber. This approach created perforated walls that worsened with pressurization. The pressurization problem was later fixed by adjusting the thickness of the print walls to 1 mm so the wall thickness had a minimum of three exterior layers of material [15]. The selected minimum allowed the slicer to avoid unnecessary print head movements that in turn created micro gaps in the print.

3.3 Block Force Testing

The 3D printed pneunet actuators were tested using a Mark-10 50 N force sensor attached upside-down to a table facing upwards with a compression plate on top, seen in Figure 6. The three actuators were each clamped to a block so their bottoms aligned with the top of the compression plate. A compressor supplied the air and a manual valve released the air after testing. Different air pressures were introduced into the actuators ranging from 15 psi to 40 psi in increments of 5 psi. The sensor recorded force data from when the air was first released into the actuators until the compressed air leaves the actuators. Each test cycle consisted of pressurizing the actuator starting at 15 psi, holding for 5 seconds, and releasing the pressure.

The actuators do not output much force below 15 psi and tend to rupture around 50 psi, therefore these pressure ranges were avoided. The larger pneunets rupture around 40 psi.

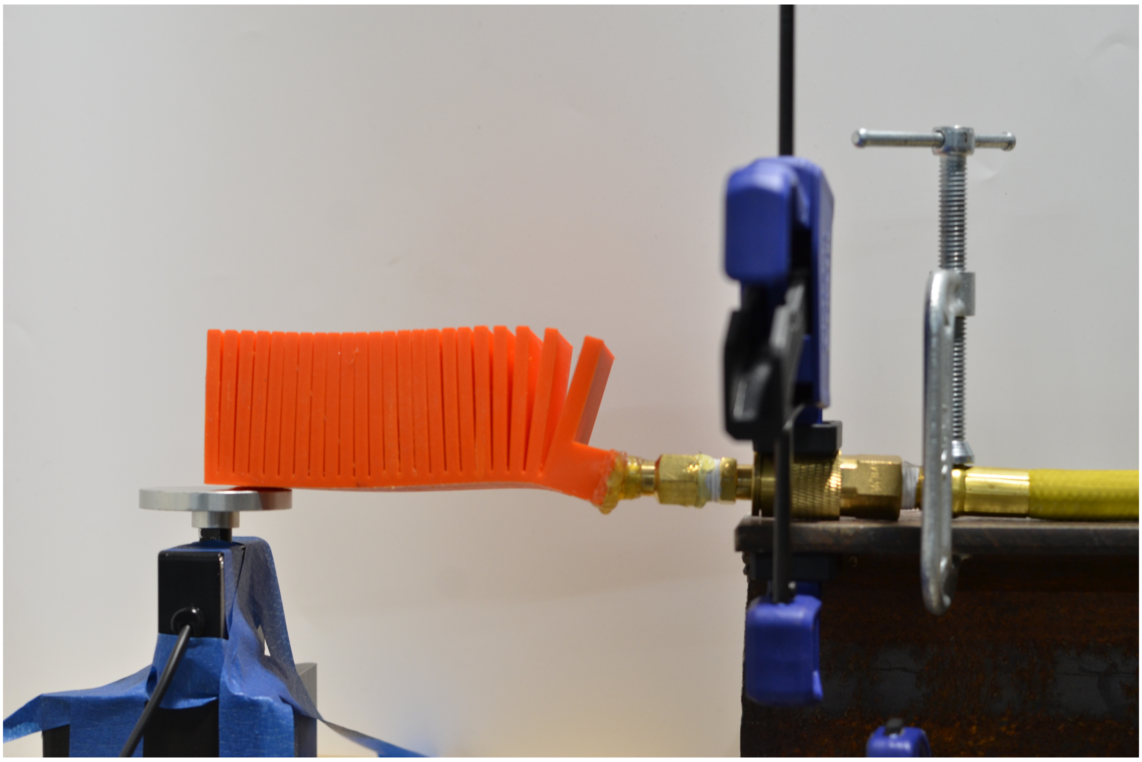

Figure 6: The figure shows the block force test setup.

3.4 Radius of Curvature Testing

The three pneunet actuators were tested for the radius of curvature. Each actuator was secured to a test apparatus in a lightbox as seen in Figure 7. Each actuator was inflated to a set pressure (15 - 40 psi), held for 5 seconds, then deflated. Each actuator was tested 4 times. A camera captured the pneunets' curvature. The images were imported into SolidWorks, where a circle was drawn to find the best fit of the radius of curvature as seen in Figure 7. The reference length of the actuator base (18 mm) was used to calculate the actual radius of curvature, as seen in Equation 1

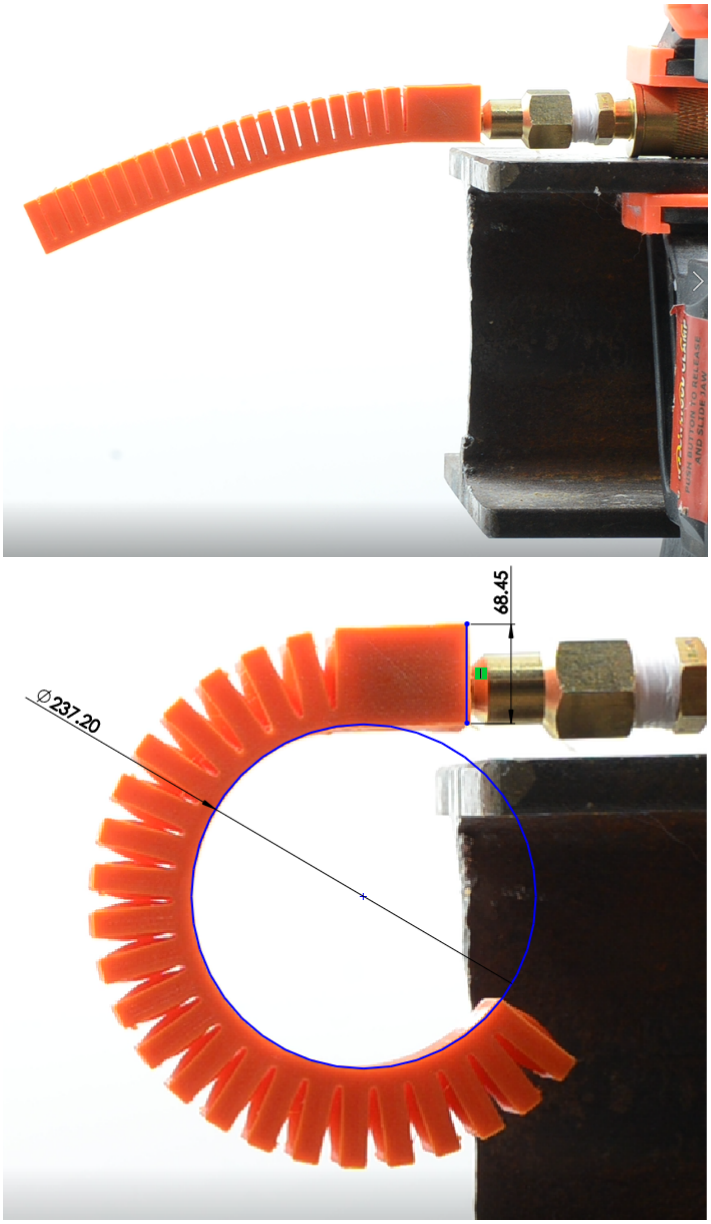

Figure 7: The figure shows the radius of curvature test set up and the SolidWorks setup

$$ActualRadius = \frac{ActualReference}{Reference} * Radius \tag{1}$$

4 Results

4.1 Block Force Testing

The blocked force tests revealed that the force output increased with pressure in a linear trend (R squared is 0.974, 0.994, 0.998 from small to large, respectively). The results in Figure 8 show each actuator's force output for all four trials.

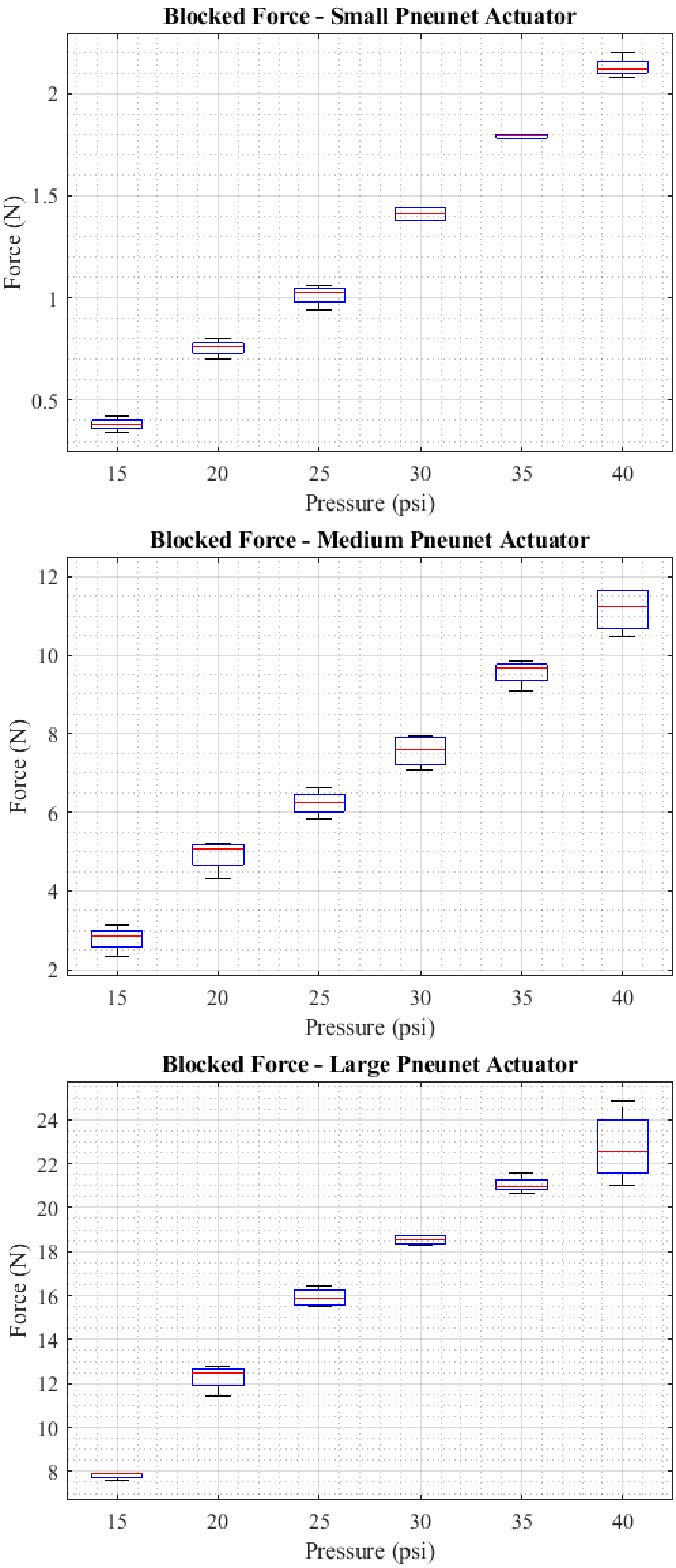

Figure 8: The block force test for all three actuators shows the range of data.

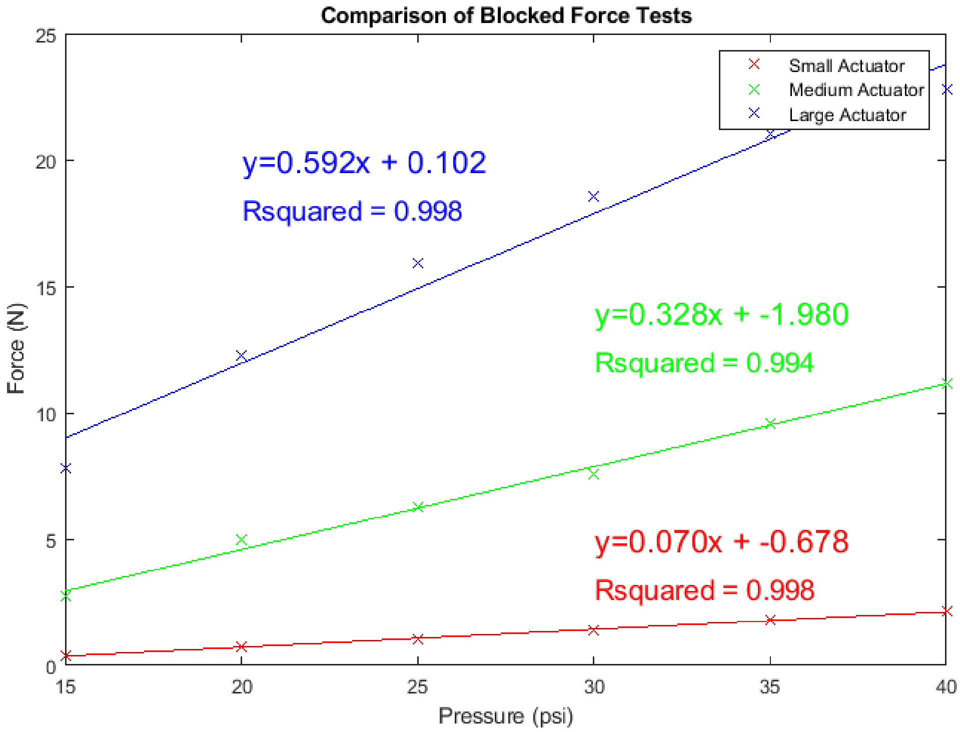

Figure 9: The three block force tests are compared accompanied by their equation of best fit and R squared values.

The three pneunets are compared in Figure 9. The force output of the actuator increases linearly as the pressure increases. The slope of the trendline for the small actuator is 0.07 N/psi with a y-intercept of -0.678 and an R squared value of 0.998. The slope of the trendline for the medium actuator is 0.328 N/psi with a y-intercept of -1.978 and an R squared value of 0.994. The slope of the trendline for the large actuator is 0.592 N/psi with a y-intercept of 0.102 and an R squared value of 0.974.

The blocked force test revealed that the force output of the 3D printed actuators increases linearly to the amount of the pressure provided by the system. The cross-sectional area of the actuators drastically increases the force output. The difference between the slopes of the trendlines for the medium and small actuators is 4.686. The difference between the slopes of the trendlines for the large and medium actuators is 0.264. The force doubles between each iteration of the actuator.

4.2 Radius of Curvature Testing

The radius of curvature testing revealed that the radius of curvature decreases with increased pressure. Figure 10 compares the radius of curvature for the three sizes of actuator with the pressures they are inflated to.

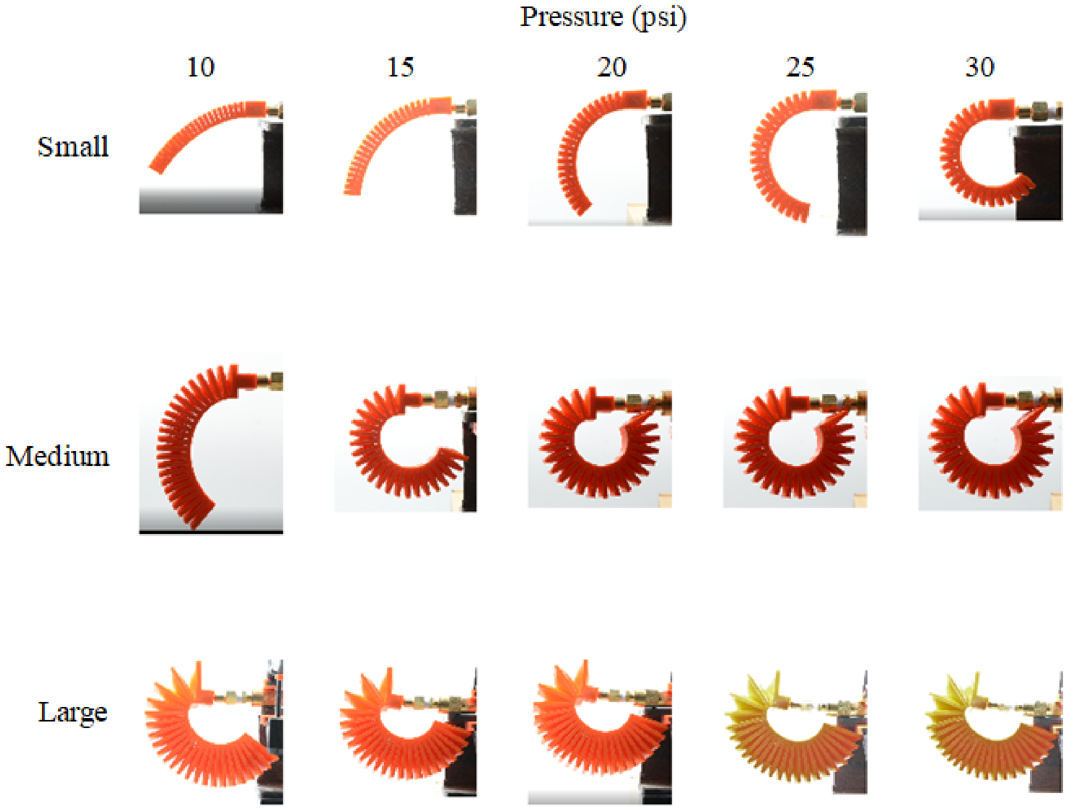

Figure 10: The radius of curvature comparison between the three cross sections.

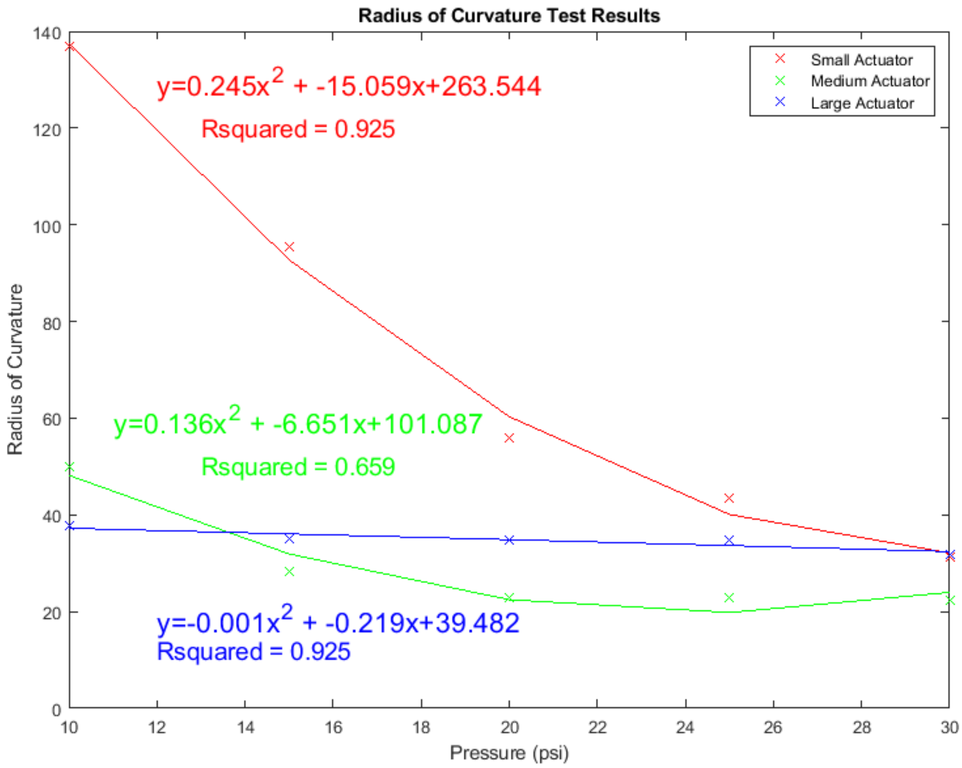

Figure 11: The radius of curvature test results

In Figure 11, the data fit is a second-order polynomial with the small, medium, and large actuators possessing an R squared value of 0.99, 0.95, and 0.86 respectively.

Pressure (PSI)	**Small Actuator Radius of Curvature (mm)**	**Medium Actuator Radius of Curvature (mm)**	**Large Actuator Radius of Curvature (mm)**
10	136.87	49.89	37.70
15	95.39	28.34	35.19
20	55.79	22.93	34.77
25	43.47	22.79	34.68
30	31.19	22.41	31.92

Table 2: The radius of curvature results

The values of the radius of curvature test are in Table 2. The radius of curvature tests demonstrates that there is more bending at the base and tip of the actuator.

5 Discussion

The 3D printed pneunet actuators move by pushing the pneunet air chamber's exterior walls into each other. At full inflation, this results in only one point touching between each of the chambers. When the chambers of these actuators are inflated, they form a triangular shape rather than the more circular shape seen in silicone [20].

(a) The TPU pneunet

(b) Martin Mann's silicone pneunet [20]

Figure 12: A comparison between the curl of the TPU actuator and the Martin Manns's silicone actuator [20]. Both pneunets' inflated chambers touch at their central point but the silicone pneunet has more surface area that touches.

The pneunet in Figure 12a, touches chambers at a single point. Meanwhile, the pneunet in Figure 12b shows the pneunet touching chambers from the base until that point. The chambers intersect at a line rather than a point. We estimate that the stiffness of the material causes the pneunet to start bending at its weakest point: the middle of the chamber. Since the silicone is more ductile, the chambers inflate in all directions while the TPU focuses on the center. More investigation will be done in future work.

5.1 Blocked Force Testing

The equation for pressure is force over area. The area remains constant while the pressure increases resulting in an increase in force. The force is generated by the chambers expanding and pushing into one another. The point where each chamber connects is where the force is transferred.

The force output varies based on the internal area of the chambers. The large pneunet had difficulties staying secured to the table and would attempt to push the connector out of the actuator. The pneunet was clamped in place and hot glue around the connector helped the pneunet maintain pressure. The small actuator has a smaller internal area that results in an output with less force.

5.2 Radius of Curvature Testing

The small actuator is the only design where the radius of curvature test setup did not affect the results. The other two actuator designs (medium and large) would bend significantly such that they would come into contact with their own connectors and attempt to push against themselves. This meant that their curvature was capped after a certain pressure.

The larger actuators have a smaller radius of curvature because their cross-sectional areas are larger. The force is transferred through the middle point of the pneunet. The point of contact between the chambers is higher up on the actuators and causes them to bend more. All actuators showed an unusual behavior where they tended to bend more on the two ends than at the middle.

6 Conclusion

The pneunet actuators were developed so they could easily be printed and attached to a gripper. The pneunets generated more force output and compliance than originally expected. These pneunets typically output more force than other silicone pneunets from my literature review. The pneunets were successful for the most part but would need improvement before becoming fully functional on an apple harvesting robot.

In the future, the connection between the soft gripper and hard pneumatic input needs to improved. The connection is the main area where air escapes and improving the connection with glue or flexible connectors would help seal it better. When the actuator is held horizontally, the weight of the pneunet drags it down which is problematic for apple picking. The actuator could be improved with a hybrid pneunet. The hybrid would consist of one or two layers of still filament followed by the TPU material. This would make the pneunet more rigid. The actuators can be assembled into a gripper for apple harvesting and tested in the field. The gripper would need to consist of three or more actuators.

7 References

[1] Zhao De-An, Lv Jidong, Ji We, Zhange Ying, and Chen Yu. "Design and Control of an Apple Harvesting Robot". In: *Biosystems Engineering* 110.2 (2011), pp. 112–122. DOI: https://doi.org/10.1016/j.biosystemseng.2011.07.005.

[2] Abhisesh Silwal, Joseph R. Davidson, Manoj Karkee, Changki Mo, Qin Zhang, and Karen Lewis. "Design, Integration, and Field Evaluation of a Robotic Apple Harvester". In: *Journal of Field Robotics* 34.6 (2017), pp. 1140–1159. DOI: https://doi.org/10.1002/rob.21715.

[3] Cameron Hohimer, Heng Wang, Santosh Bhusal, John Miller, Changki Mo, and Manoj Karkee. "Design and Field Evaluation of a Robotic Apple Harvesting System with A 3D-Printed Soft-Robotic End-Effector". In: *Transactions of the ASABE* 62.2 (2019), pp. 405–414. DOI: https://doi.org/10.13031/trans.12986.

[4] Jasper Brown, and Salah Sukkarieh. "Design and Evaluation of a Modular Robotic Plum Harvesting System Utilising Soft Components". In: *Journal of Field Robotics* 38.2 (2021), pp. 289–306. DOI: https://doi.org/10.1002/rob.21987.

[5] Cecelia Laschi, Matteo Cianchetti, Barbara Mazzolai, Laura Margheri, Maurizio Follador, and Paolo Dario. "Soft Robot Arm Inspired by the Octopus". In: *Advanced Robotics* 26.7 (2012), pp. 709–727. DOI: https://doi.org/10.1163/156855312X626343.

[6] Alex Zatopa, Steph Walker, and Yigit Menguac. "Fully Soft 3D-Printed Electroactive Fluidic Valve for Soft Hydraulic Robots". In: *Soft Robotics* 5.3 (2018), pp. 258–271. DOI: https://doi.org/10.1089/soro.2017.0019.

[7] Thomas Wallin, James Pikul, and Robert Shepherd. "3D Priting of Soft Robotic Systems". In: *Nature Reviews Materials* 3.6 (2018), pp. 84–100. DOI: https://doi.org/10.1038/.

[8] Jun Li, Manoj Karkee, Qin Zhang, Kehui Xiao, and Tao Feng. "Characterizing Apple Picking Patterns for Robotic Harvesting". In: *Computer and Electronics in Agriculture* 127 (2016), pp. 633–640. DOI: http://dx.doi.org/10.1016/j.compag.2016.07.024.

[9] Yufei Hao, Shantonu Biswas, Elliot Wright Hawkes, Tianmiao Wang, Mengjia Zhu, Li Wen, and Yon Visell. "A Multimodal, Enveloping Soft Gripper: Shape Conformation, Bioinspired Adhesion, and Expansion-Driven Suction". In: *IEEE Transactions on Robotics* 37.2 (2021), pp. 350–362. DOI: http://doi.org/10.1109/TRO.2020.3021427.

[10] Yingtian Li, Yonghua Chen, Yang Yang, and Ying Wei. "Passive Particle Jamming and Its Stiffening of Soft Robotic Grippers". In: *IEEE Transactions on Robotics* 33.2 (2017), pp. 446–455. DOI: https://doi.org/10.1109/TRO.2016.2636899.

[11] Shuguang Li, John J. Stampfli2, Helen J. Xu, Elian Malkin, Evelin Villegas Diaz, Daniela Rus, and Robert J. Wood. "A Vacuum-driven Origami "Magic-ball" Soft Gripper". In: *IEEE International Conference on Robotics and Automation* (2019). DOI: http://hdl.handle.net/1721.1/120930.

[12] Joseph Davidson, Abhisesh Silwal, Manoj Karkee, Changki Mo, and Qin Zhang. "Hand-Picking Dynamic Analysis for Undersensed Robotic Apple Harvesting". In: *Transactions of the ASABE* 59.4 (2016), pp. 745–758. DOI: https://doi.org/10.13031/trans.59.11669.

[13] Yi Sun, Yun Seong Song, and Jamie Paik. "Characterization of Silicone Rubber Based Soft Pneumatic Actuators". In: *RSJ International Conference on Intelligent Robots and Systems* (2013), pp. 4446–4453. DOI: https://doi.org/10.1109/IROS.2013.6696995.

[14] Jahan Zeb Gul, Memoon Sajid, Muhammad Muqeet Rehman, Ghayas Uddin Siddiqui, Imran Shah, Kyung-Hwan Kim, Jae-Wook Lee, and Kyung Hyun Choi. "3D Printing for Soft Robotics - A Review". In: *Science and Technology of Advanced Materials* 19.1 (2018), pp. 243–262. DOI: https://doi.org/10.1080/14686996.2018.1431862.

[15] Gianni Stano, Luca Arleo, and Gianluca Percoco. "Additive Manufacturing for Soft Robotics: Design and Fabrication of Airtight, Monolithic Bending PneuNets with Embedded Air Connectors". In: *Micromachines* 11.5 (2020), p. 485. DOI: https://doi.org/10.3390/mi11050485.

[16] Zhongkui Wang, and Shinichi Hirai. "Soft Gripper Dynamics Using a Line-Segment Model With an Optimization-Based Parameter Identification Method". In: *IEEE Robotics and Automation Letters* 2.2 (2017), pp. 624–631. DOI: https://doi.org/10.1109/LRA.2017.2650149.

[17] Kanygul Chynybekova, and Soo-Mi Choi. "Flexible Patterns for Soft 3D Printed Fabrications". In: *Symmetry (Basel)* 11.11 (2019), p. 1398. DOI: https://doi.org/10.3390/sym11111398.

[18] *NinjaFlex 3D Printer Filament (85A)*. URL: https://ninjatek.com/shop/ninjaflex/.

[19] Yu Yanagihara, Noboru Osaka, Sohgo Iimori, Satoshi Murayama, and Hiromu Saito. "Relationship between modulus and structure of annealed thermoplastic polyurethane". In: *Materials Roday Communications* 2 (2015), e9–e15. DOI: https://doi.org/10.1016/j.mtcomm.2014.10.001.

[20] Martin Manns, Jorge Morales, and Peter Frohn. "Additive Manufacturing of Silicone Based PneuNets as Soft Robotic Actuators". In: *Procedia CIRP* 72 (2018), pp. 328–333. DOI: https://doi.org/10.1016/j.procir.2018.03.186.